Journal Name

ARTICLE TYPE

Cite this: DOI: 10.1039/xxxxxxxxxx

Role of electrostatic interactions on the adsorption kinetics of nanoparticles at fluid-fluid interfaces†

Venkateshwar Rao Dugyala,[a] Jyothi Sri Muthukuru,[a] Ethayaraja Mani,[a] Madivala G Basavaraj*[a]

Received Date
Accepted Date

DOI: 10.1039/xxxxxxxxxx

www.rsc.org/journalname

The adsorption of particles to the fluid-fluid interface is a key factor for the stabilization of the fluid-fluid interfaces such as those found in emulsions, foams and bijels. However, for the formation of stable particle-laden interfaces, the particles must migrate to the interface from the bulk. In the context of Pickering emulsion stabilization, it has recently been shown that the charge on the particles plays an important role in the movement of particles to the interface and hence in emulsion stabilization (Wang *et al.*). To further investigate this phenomena, we study the effect of charge density of particle on the adsorption kinetics of particles to the oil-water interface. We use monodisperse silica nanoparticles and the electrostatic interaction between the particles is tuned by the addition of monovalent salt. By suspending a drop of aqueous dispersion of nanoparticles in decane medium, the adsorption dynamics of particles to the decane-water interface is studied using the dynamic surface tension measurements. When the particles are highly charged (low salt concentration), a negligible change in the interface tensions is observed indicating almost no particles adsorbed. These results show that the charged particles experience an energy barrier when they approach the interface. But when the particles are weakly charged (high salt concentration), a significant drop in interfacial surface tension is observed indicating the migration and adsorption of particles to the decane-water interface. We estimate the effective diffusivity of particles to the interface by analyzing the initial decay in the measured surface tension with particle laden drops containing different amount of salt using the modified Ward and Tordai theory. This effective diffusivity is used to calculate the energy barrier obtained for adsorption of particles to the interface. The energy barrier from the analysis of dynamic surface tension data agree well with the concept of image charge repulsion which inhibits the adsorption of highly charged particles to the interface.

1 Introduction

The spontaneous or forced adsorption of particles to the liquid-liquid or liquid - air interface is one amongst many strategies to create different functional materials using, for example, Pickering emulsion [1–5], foam [6–9] and bijel [10–12] structures as templates. These functional materials have diverse applications in different fields such as oil recovery, drug delivery, porous catalyst and multi porous membranes. Crucial to the design of these novel functional materials is the migration and deposition of particles to the interfaces and the stabilization of incompatible interfaces. To create stable particle laden interfaces, it is a general practice to add certain additives such as surfactants or electrolytes. For example, the addition of salt is known to effect Pickering emulsion stabilization. The role of electrostatic interactions and the mechanism that leads to the formation of stable particle-laden interface with the addition of salt is poorly understood.

In general, to form Pickering emulsions external energy is used to create new interface either via manual or mechanical mixing. This applied energy will facilitate the migration of the particles from the bulk to the newly created interface. It has been shown recently that in-order to form stable particle stabilized emulsions, the magnitude of external energy required is higher if the particles are highly charged.[1] This has been attributed to the image charge induced energy barrier that must be overcome when the particles approach near to the interface. The estimation of this energy barrier is important because it also affects the kinetics of

[a] *Polymer Engineering and Colloid Science Lab (PECS Lab), Department of Chemical Engineering, Indian Institute of Technology Madras, India; E-mail: basa@iitm.ac.in*

† Electronic Supplementary Information (ESI) available: [early time plots for different salt concentration]. See DOI: 10.1039/b000000x/

‡ Additional footnotes to the title and authors can be included *e.g.* 'Present address:' or 'These authors contributed equally to this work' as above using the symbols: ‡, §, and ¶. Please place the appropriate symbol next to the author's name and include a `\footnotetext` entry in the the correct place in the list.

adsorption of particles to the interface. In this article, we provide a simple methodology for the estimation of this energy barrier through dynamic surface tension measurements.

Planar particle monolayers or two-dimensional particle laden flat interfaces are widely studied in literature. For example, ordering of particles in the monolayer, structural transitions, aggregation kinetics and influence of particle shape on the structural arrangement have been widely investigated.[13–18] It must be noted that in these studies, particles in a suitable medium are spread typically using a micro-syringe such that particles invariably accumulate at the interface. This enables the study of various phase transitions and structure-property correlation in particle monolayer at flat interfaces. Comparatively, however, few authors have studied the adsorption kinetics of particles to the fluid-fluid interfaces.[19–26] In most of the studies, authors investigated the adsorption kinetics by using the pendent drop technique, which is a widely used method to investigate the adsorption kinetics of surfactants to interfaces. Nanoparticles with different stabilizers (trin-octylphosphine oxide (TOPO)-stabilized CdSe nanoparticles or alkaline caped gold nanoparticle) have been used to study the effect of particle concentration and size on the adsorption kinetics.[21,22,27] From these experiments, the authors observed an increase in the adsorption rate with increase in particle concentration. Recently, Nelson *et al.* investigated the adsorption of iron oxide-poly (ethylene glycol) core shell particle to the water-decane interface.[25] The particle adsorption rate is observed to be proportional to the bulk concentration and at the maximum coverage the particle-laden interface still behaved as a fluid. The use of pendant drop technique for dynamic and equilibrium surface tension measurements showed significant higher interfacial activity of Janus nanoparticles of controlled amphiphilicity.[24] The increase in surface tension drop with gold nanoparticles modified using dodecanethiol (DDT) or octadecanethiol (ODT) was attributed to the hydrophobic nature of the grafted gold nanoparticles. More recently, adsorption of soft microgel particles has been investigated.[20] While diffusion of the particles from bulk to the interface controls the adsorption of these particles at short times, at long times, the crowding of articles at the interface creates a entropic barrier for newer particles to adsorb onto the interface.

Though the adsorption of particle to the interface is thermodynamically favored, their adsorption kinetics depends on a number of parameters. Typically, the adsorption kinetics of nanoparticles measured via the pendant drop method is analyzed to understand the effect of various parameters on adsorption kinetics. The early and late stage adsorption process monitored via the dynamic surface tension (DST) experiments is generally modeled using the Ward and Tordai (1946) theory.[28] According to this theory the kinetic process depends on the particle size and concentration - that is adsorption is purely diffusion controlled. In the absence of any external energy barrier, the time required for a particle to reach the interface from the bulk depends only on the particle diffusivity because this theory assumed instantaneous adsorption to the interface. However, in the presence of an energy barrier, the rate of adsorption of particles to the interface decreases and therefore both diffusion and energy barrier become important. Several theories were put forward to include diffusion and adsorption kinetics in the overall kinetics of adsorption, especially for surfactant adsorption studies.[29–32]

Recently, Bizmark *et al.*, studied the kinetics of adsorption of ethyl cellulose nanoparticles at water-air interface.[19] The asymptotic solutions of Ward and Tordai theory in the limit of $t \to 0$ and $t \to \infty$ were used to explain their experimental data on the reduction of surface tension with time. In particular, for $t \to 0$, in other words the initial decay of surface tension is given by

$$\gamma = \gamma_0 - 2N_A C_0 \Delta E \sqrt{\frac{Dt}{\pi}} \tag{1}$$

In this equation, γ is interfacial tension at any given time t , γ_0 is the pure water-decane interfacial tension, N_A is the Avogadro number, C_0 is the initial bulk concentration of particles and ΔE is the detachment energy of the particle. The detachment energy of the particle is defined as

$$\Delta E = \pi r^2 \gamma_0 (1 - |\cos\theta|)^2 \tag{2}$$

with r as radius of the particles and θ as three phase contact angle. Bizmark *et al.* used eqn1 to fit the initial γ vs $\sqrt{t}$ data with ΔE as the fitting parameter for several initial concentration of particles C_0. While the authors conclude that ΔE depends on particle concentration, by definition, ΔE is a function of only interfacial tension, particle size and contact angle.The above equation also assumes that the adsorption of particles to the interface is instantaneous. In their study, adsorption of particles to the interface is dominated by the hydrophobic attraction between particle and interface interactions electrostatic repulsions are not significant. However, when the particles are highly charged, the contribution to repulsive interactions due to electrostatic interaction between particle and interface, particle and image charge, and repulsion between approaching particle and particles already adsorbed at the interface are to be considered. Previous studies have not considered these effects in understanding adsorption of nanoparticles examined via dynamic surface tension measurements

In this work we investigate the effect of particle charge on the adsorption kinetics. From the study of dynamic surface tension of aqueous drops containing charge particles suspended in an oil medium, we demonstrate the role of particle charge on their adsorption to water-oil interface. Aqueous suspensions containing mono-disperse silica particles of known surface charge density are used in all experiments. When the particles are highly charged, the change in the surface tension with time is negligible. However, as the particle charge is reduced by the addition of monovalent salt, the observed decrease in the surface tension is significant. This drop in surface tension is attributed to the adsorption of particles to the oil-water interface. By analyzing the initial drop in the surface tension measured as a function of salt concentration using the Ward and Tordai theory, we calculate the effective diffusivity of particles to the interface. The effective diffusivity is found to be about few orders of magnitude less than Stoke-Einstein's diffusivity indicating the existence of an energy barrier for the adsorption of particles to the decane-water interface. The energy barrier is found to decrease with increase in salt concentration. The energy barrier from the analysis of dynamic surface

tension (DST) data is compared with the calculation of the overall DLVO and image charge interactions close to the interface. The energy barrier from the analysis of DST measurements agree well with DLVO calculations when the concept of image charge repulsion is incorporated. The effect of particle concentration on the adsorption kinetics is also studied and found that $\Delta\gamma \propto C$.

2 Methods

Charge stabilized (negative) mono-disperse silica nanoparticle suspension (Ludox SM30) was obtained from the Sigma Aldrich. This suspension was purchased as an aqueous dispersion containing 30 % particles by weight. The silica suspension was used as received. The hydrodynamic diameter of these particles as measured by dynamic light scattering technique was 10nm. For adsorption studies, decane (Merck, India) was used as oil medium. The decane was treated with activated alumina to remove water soluble impurities if any. A series of silica nanoparticle suspensions of different weight fraction ranging from 0.25 to 1 wt% were prepared from the stock Ludox SM30 suspensions (30wt%) by dilution with the deionized water from MilliQ (18.2 MΩ.cm). In order to screen the surface charge of particles, the monovalent NaCl salt was used. The electrophoretic mobility of particle was measured with electrophoretic dynamic light scattering (DLS, nanopartica, Horiba, Japan). From the mobility data the particle zeta potential was calculated by using Smalchousky equation.

The pendant drop method was used to measure the interfacial tension as a function of time. The dynamic interfacial tension of ludox suspension-decane was measured with the Goniometer (GBX, Digidrop, France). All experiments were conducted at a constant temperature of $28 \pm 2^0 C$. Two types of experiments were performed. In first set of experiments, the NaCl concentration was varied (from 0.001M to 0.1M), but the number of particles in the suspension was kept constant (at 1 wt %). In the second set of experiments, the number of particles in the suspension was systematically increased (0.25 to 1 wt%) at a fixed NaCl concentration. The experimental setup has been shown in Fig. 1. A transparent rectangular disposable plastic cuvette was filled with decane. A suspension drop containing charged silica particles at known salt concentration was suspended in the decane medium with the help of a syringe. A 20 μl suspension droplet was used in all the experiments. A series of time sequence images of the drop were captured for 2500 sec at frame rate of 30 images per minute. The captured images were used to calculate the interfacial tension by the drop shape analysis wherein the contour of drop was fitted with the Young Laplace equation to determine the interfacial tension. All the experiments were repeated at least for 3 times for consistency.

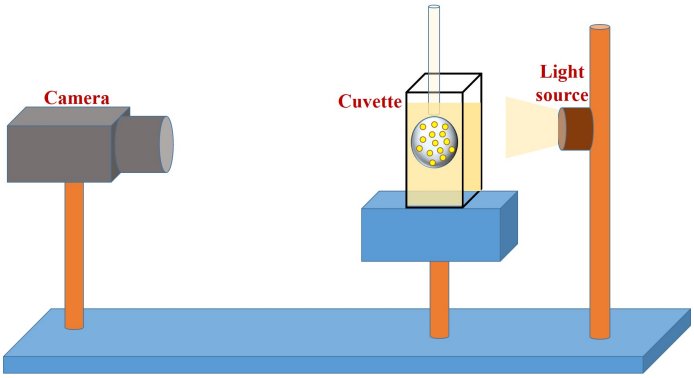

Fig. 1 The schematic of experimental setup for dynamic surface tension (DST) measurements using the pendant drop method. A Ludox SM30 silica nanoparticle suspension drop suspended in a continuous decane medium is imaged with the help of a CCD camera.

3 Results and discussion

3.1 Effect of charge density of particle on adsorption kinetics

In all the experiments the concentration of particles in the aqueous suspension drop is fixed at 1wt%. The surface charge on the particle is screened by the addition of appropriate quantity of sodium chloride (NaCl). The concentration of NaCl in the drop is varied from 0.001 M to 0.1 M. This helps us study the sole influence of particle charge effect on adsorption dynamics as all other conditions are identical in this concentration of salt and all the particles well dispersed. Initially, control experiments are carried out with pristine water drop without any particles and water drop containing 1wt% particles without any salt. The dynamic surface tension data recorded from the Pendant drop technique is shown in Fig. 2. In the control experiment without particles and salt i.e., for the decane-water interface the interfacial tension is almost constant. A negligible change in the interfacial tension is observed which may be due to the presence of small amount of water soluble impurities that are probably not removed during the treatment of decane with activated alumina. Similarly, with 1wt% suspension drop without any NaCl that is when the drop contains highly charged particles, there is almost no change in the interfacial tension. However, as the concentration of NaCl in the suspension is systematically increased, the dynamic interfacial tension data showed a sharp decrease as shown in Fig. 2. From the Fig.2, a significant change in the interface surface tension is observed with time when the salt concentration is high (0.1M).

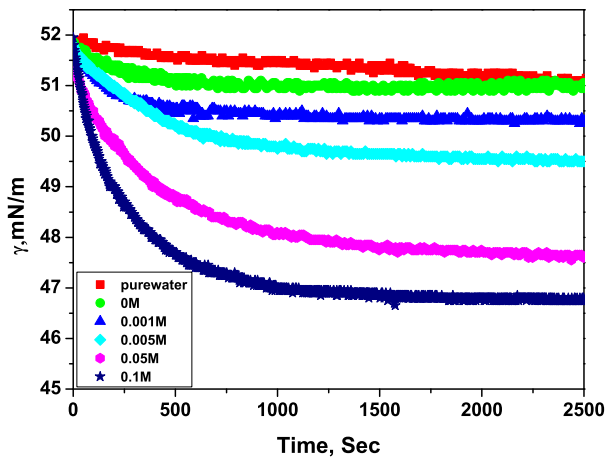

Fig. 2 The dynamic surface tension of decant-aqueous silica nanoparticle suspension as a function of NaCl concentration. The particle concentration is 1wt% in all the experiments. A significant decrease in interfacial tension can be seen as the salt concentration is increased.

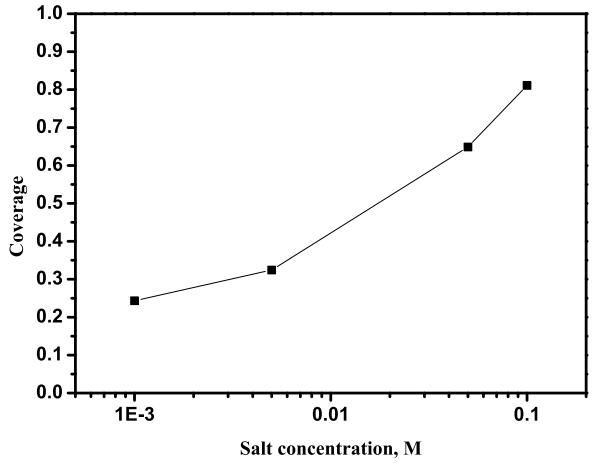

Fig. 3 Particles coverage at interface for different salt concentrations. The coverage is calculated at t=2500 sec. The particle coverage is increased as the salt concentration increased. The line is a guide to eye.

The decrease in the interfacial tension is associated with the adsorption of particles to the decane-water interface. The decrease in interfacial tension is significant at initial time and thereafter, the interfacial tension drop is very sluggish reaching a plateau at later times. In case of lowest salt condition used (0.001M), the change in the interfacial tension is very similar to the case of salt free suspension. The surface coverage of the particle at the interface is calculated by using eqn3.

$$\Delta E = \frac{\gamma_0 - \gamma_t}{\Phi_t} \pi r^2 \sin^2\theta \tag{3}$$

where, γ_0 is the interfacial tension at $t = 0$, γ_t is interfcial tension at any given time t , ΔE is the particle detachment energy from the interface, Φ_t is the particle coverage at interface, θ is the contact angle between particle and interface and r is the particle radius. The particle detachment energy from the interface was calculated from eqn 2. Since the actual position of nanoparticles with respect to the interface was difficult to measure, the contact angle for micron sized particles that has been reported was used ($\theta = 38^0$).[33,34] The calculated particle coverage for different salt concentrations is shown in Fig (3). From the Fig. 3, as the salt concentration is increased, the particle coverage increased. To conclude, these experiments show the particles adsorption to the fluid-fluid interface strongly depends on the concentration of NaCl and hence on the particle surface charge.

3.2 Modeling of nanoparticle adsorption

In the pendant drop experiments, unlike emulsification process, no mechanical energy is provided externally to promote particle adsorption to the interface. That is the particles approach the interface solely due to their diffusivity. Generally, the adsorption of particles at interface is controlled by either diffusion controlled or energy barrier controlled model or a combination of both. At initial times ($t \to 0$), the adsorption is limited by the diffusion process as the interface is free of particles. That is - there is no hindrance for the particles to adsorb at interface and once particles adsorb to the interface it is very unlike that it detaches from the interface as a result of the high detachment energy ($\sim 50 k_B T$). Therefore, we use modified diffusion controlled (Ward and Tordai) theory to model the early time adsorption process. We can infer from the experimental results in Fig. 2 that with the addition of salt, there is adsorption of particles to the interface which is associated with the drop in interfacial tension. Thus, it clearly indicates the presence of an energy barrier as the particles approach near to the interface. This energy barrier (of all kinds-particle-interface DLVO interactions and image charge repulsion) will effect the particles flux to the interface. To include the energy barrier effects on adsoprtion process, we replace the particle diffusivity D with the effective diffusion coefficient D_{eff} in the eqn 1. The effective diffusivity model is previously used for the protein adsorption at interface and diffusion of charged particle in porous materials.[35–37] We therefore calculate the effective diffusivity of the particles by modeling the early time dynamic surface tension data using the adsorption kinetic model (4)

$$\gamma = \gamma_0 - 2N_A C_0 \Delta E \sqrt{\frac{D_{eff} t}{\pi}} \tag{4}$$

Where, D_{eff} is the effective diffusion constant.

For further analysis, the early time DST data from 0 to 100 sec was used. A typical plot showing the early time DST data fitted

][H]

Table 1 The fitted parameter for the suspension contains 1 wt% particles with different salt concentration. The effective diffusion and energy barrier is calculated from the model. The actual diffusion of the particle is 4.98 $\times 10^{-11} m^2/s$

Salt concentration (M)	Fitting parameter p1 (mN/m)	Fitting parameter p2 (mN/m^2)	D_{eff} m^2/s	U/k_BT (from eq(5)
0.001	51.86	0.0662	1.90 $\times 10^{-15}$	10.20
0.005	51.96	0.0706	2.17 $\times 10^{-15}$	10.04
0.05	51.73	0.1299	7.34 $\times 10^{-15}$	8.82
0.1	52.3	0.2348	2.40 $\times 10^{-14}$	7.63

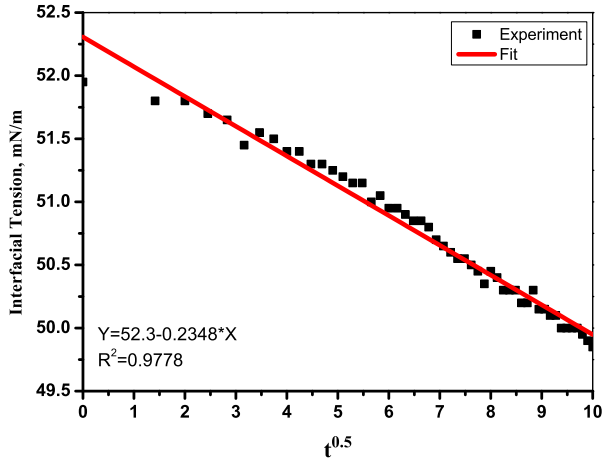

Fig. 4 Plot between early time DST data (from 0 to 100 sec) of suspension contains 1wt% particles and 0.1M NaCl concentration vs $\sqrt{t}$. The solid line represents fitting of early time adsorption kinetics model with eqn 4. The fitting parameters and R^2 values are shown in the plot.

with eqn 4 for a drop containing 1wt% suspension and 0.1M salt concentration is shown in Fig.4. By using the fitting parameters the effective diffusivity of the particles (D_{eff}) was calculated. The calculated effective diffusivity was $2.40 \times 10^{-14}\ m^2/s$, about three order of magnitude lower than Stokes-Einstein particle diffusivity of $4.98 \times 10^{-11}\ m^2/s$. As the concentrationn of salt in the suspension is increased, the effective diffusivity is found to increase. Table 1 shows the effective diffusivity data calculated at the NaCl concentrations studied. We attributed the change in the effective diffusivity to the energy barrier for adsorption of particles at the interface as the particles. The effective diffusivity D_{eff} due to the presence of an energy barrier U is related to the bare diffusion coefficient D_0 (without any adsorption barrier) is given by

$$D_{eff} = D_0 \exp\left(-\frac{U}{k_B T}\right) \quad (5)$$

The actual diffusivity of the particle is calculated by using the Stokes-Einstein equation. By using the eqn 5 the energy barrier (U) was calculated from the effective diffusivity values. The energy barrier at 0.1M salt concentration was $7.63 k_B T$. The effective diffusivity and energy barrier at different salt concentration has been tabulated in Table 1. From the Table 1, as the salt concentration is increased, the energy barrier decreased. At low salt concentration, the thermal energy of the particles is not enough to overcome the energy barrier. Since the particles used are electrostatically stabilized, the energy barrier is likely to be of electrostatic origin and therefore we calculate the DLVO interactions near the interface.

3.3 Overall DLVO calculation

The energy barrier obtained from modeling the time variation of interfacial tension is compared with the possible charge induced energy barrier for particle adsorption to decane-water interface. We calculated the overall DLVO interactions in the vicinity of the interface. It is known that under experimental conditions, the interface is negatively charged.[38] The overall DLVO interactions near the interface is summation of 1) the van der Waals interaction between the particles and charged interface 2) the electric double layer interaction due to surface charge of the interface and the particles. Under experimental conditions, both the particles and the interface are always negatively charged (see Table 2), therefore, it can be argued that the repulsive barrier is due to particle-interface repulsion.

Table 2 The Ludox SM30 silica nanoparticles zeta potential as a function of salt concentration. The interface zeta potential is obtained from the literature.[38]

Salt concentration M	Particle zeta potential (mV)	Interface zeta potential (mV)
0	-63.6	
0.001	-48.9	-60
0.005	-40	-45
0.05	-24.5	-30
0.1	-15	-20

However, it was recently shown that a repulsive barrier still exists when the particles and interface are oppositely charged - that is when particles are positively charged and interface is negatively charged. This repulsive barrier was attributed to the image charge effects. In the overall DLVO calculations, we therefore included the image charge effects as well. In the case of liquid drop containing charged particles suspended in another fluid, the origin of image charge effect is due to the difference in the dielectric constants of the fluids across the interface. The image charge zeta potential is calculated by using the eqn 6.[1]

$$\Psi_{image} = \Psi_{particle}\frac{\varepsilon_1 - \varepsilon_2}{\varepsilon_1 + \varepsilon_2} \quad (6)$$

In eqn 6, ε_1 is the dielectric constant of the medium which contains the charged particle and ε_2 is the dielectric constant of the particle free medium. From the eqn 6, when a charged particle present in a high dielectric medium such as water ($\varepsilon_1 \approx 78$) approaches an interface across which a low dielectric medium is present (decane $\varepsilon_2 \approx 2$) , the particles experience a repulsion due to a like-charged particle present across the interface (See Fig. 5). However, the image charge interaction can also be attractive. If the particle resides in a low dielectric medium, the image charge according to eqn 6 is opposite in sign, therefore image charge interactions are always attractive. However, it is difficult to have particles in low dielectric medium in a charged state. The overall DLVO interaction of particles close to the interface therefore is $U_{total} = U_{vdw} + UE_{p-int} + UE_{p-image}$ The nature of the DLVO interaction between the particle and the interface can be considered as interaction between a spherical particle and a flat plate. The van der Waal interaction between the particle and interface is calculated by using the eqn 7.[39]

$$U_{vdw} = -\frac{A}{6}\left[\frac{r}{h} + \frac{r}{h+2r} + \ln\left(\frac{h}{h+2r}\right)\right] \quad (7)$$

Where, A is the effective Hamaker constant, r is the particle radius and h is the surface to surface distance between the particle and interface. The effective Hamaker constant is calculated from the mixing rule as $A \approx \sqrt{A_{oil} - A_{water}}\sqrt{A_{particle} - A_{water}}$ where, A_{oil} is the Hamaker constant for the oil $(5 \times 10^{-20} J)$, A_{water} is the Hamaker constant for water $(4 \times 10^{-20} J)$ and $A_{particle}$ is Hamaker constant of silica particles $(6.5 \times 10^{-20} J)$. The effective Hamaker constant was calculated to be $\approx 1.3 \times 10^{-21} J$.

To model electrostatic double layer (EDL) interactions, a linear superposition approximation (LSA) method proposed in the literature was used as the interaction energies estimated with LSA are more realistic than the predictions of constant potential and constant charge models. The EDL interaction between the particle-interface and particle-image particle was calculated using eqn 8 and eqn 10, respectively.[40]

$$UE_{p-int} = UE_{p-int}(h) + UE_{p-int}(h+2r) + \frac{64\pi\varepsilon}{k}\left(\frac{k_B T}{ze}\right)^2 \gamma_p \gamma_{int}[-e^{-kh} + e^{-k(h+2r)}] \quad (8)$$

$$UE_{p-int}(h) = 64\pi\varepsilon r\left(\frac{k_B T}{ze}\right)^2 \gamma_p \gamma_{int}[-e^{-kh}] \quad (9)$$

$$UE_{p-image}(h) = 32\pi\varepsilon r\left(\frac{k_B T}{ze}\right)^2 \gamma_p \gamma_{image}[-e^{-2kh}] \quad (10)$$

$$\gamma_p = \tanh\left(\frac{ze\Psi_p}{k_B T}\right) \quad (11)$$

$$\gamma_{int} = \tanh\left(\frac{ze\Psi_{int}}{k_B T}\right) \quad (12)$$

$$\gamma_{image} = \tanh\left(\frac{ze\Psi_{image}}{k_B T}\right) \quad (13)$$

Where, $\varepsilon = \varepsilon_0\varepsilon_r$, ε_0 is the dielectric permittivity of the vacuum, ε_r is the dielectric constant of water, r is the particle radius,h is the surface to surface distance, k^{-1} is the Debye length, Ψ is the surface potential, k_B is the Boltzmann constant, z is the electron valance, e is the electron charge and T is the temperature. In equations (8) to (13), the subscript of p indicates particle, *int* indicates interface (in this case oil-water interface), *image* denotes image charge. The average particle size of 10 nm was used for the calculation of interaction potential. At low salt concentration (0.001M), the individual contributions and the overall DLVO interaction energy as a function of separation distance is showed in Fig.6. From the Fig.6, the EDL interactions between the particle-interface and particle-image charge are repulsive and van der Waals interaction is attractive. The overall DLVO interaction en-

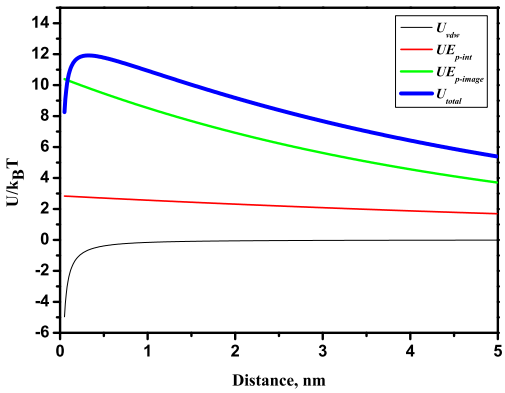

Fig. 6 The contribution of various interactions to the overall DLVO particle-interface interaction energy at 0.001M NaCl concentration. The overall (U_{total}) energy barrier is more near the interface. At low salt concentration the image charge EDL interactions are dominating.

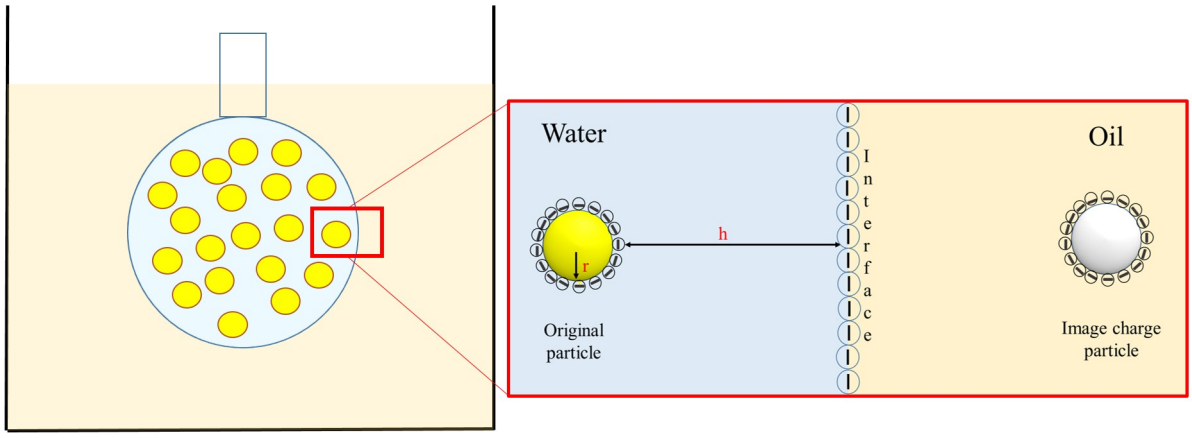

Fig. 5 Schematic diagram of charge particle near the interface and image charge. The particle radius is r and h is the distance between the particle and interface. The original particle feels its image charge in oil medium at the same distance from the interface.

ergy shows an energy barrier of $11.93k_BT$. The image charge repulsive energy is higher than the particle-interface repulsion energy and these interactions dominate at small surface to surface separation distance. So the thermal energy of the particle is not sufficient to overcome the energy barrier. Thus particles do not reach the interface and hence no adsorption. When the surface charge was screened by the addition of 0.05 M NaCl, the energy barrier reduces to $5.65k_BT$ (See Table 3). Correspondingly, a small decrease in surface tension was observed when 0.05 M NaCl was added.

Table 3 A comparison of the energy barrier calculated from early stage DST data and overall DLVO interactions. The effective diffusivity used in predicting energy barrier is also shown. The actual diffusion of the particle is $2.37 \times 10^{-12} m^2/s$.

Salt concentration M	D_{eff} m^2/s	U/k_BT (from eq(5))	U/k_BT (DLVO+image)
0.001	1.90×10^{-15}	10.20	11.93
0.005	2.17×10^{-15}	10.04	10.74
0.05	7.34×10^{-15}	8.82	5.65
0.1	2.40×10^{-14}	7.63	1.70

However, at a higher salt concentration of 0.1M NaCl, the overall DLVO interaction energy barrier as shown in Fig. 7 is small and comparable to the thermal energy of the particles.

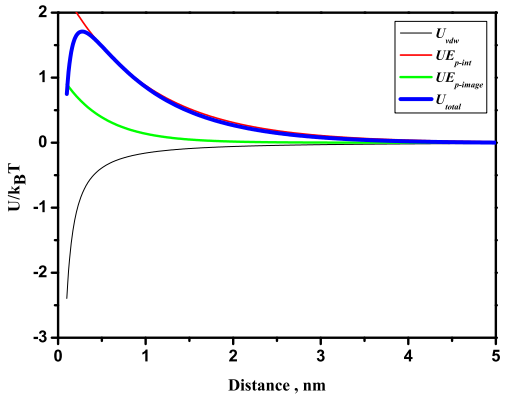

Fig. 7 The contribution of various interactions to the overall DLVO particle-interface interaction energy at 0.1M NaCl concentration. The overall interaction (U_{total}) energy barrier is small near the interface.

The energy barrier calculated was $1.70k_BT$. Therefore, the particles were found to adsorb readily to the oil-water interface as confirmed by the DST measurements (see Fig. 2). The addition of salt screens the surface charge of the particle and oil-water interface (Table 2). As the overall energy barrier is small, the thermal energy of the particles is sufficient to overcome this energy barrier. The energy barrier estimated from the DST data and the energy barrier calculated by considering the contribution of image charge repulsion to the overall DLVO at different salt concentration are given Table 3. While the energy barriers do not match quantitatively, a similar trend can be seen. It was observed that the energy barrier from the two approaches monotonically decrease with increase in NaCl concentration, which is expected. The discrepancy is probably due to the fact that only pair wise interaction between particle and interface was used in overall DLVO calculations. However, the DST measurements are a result of multi-particle interactions. The incorporation of multi-body interactions and size polydispersity in the overall DLVO interaction calculation would be more appropriate. At higher salt concentration the presence of aggregates that have lower diffusivity may

also contribute to this deviation.

3.4 Effect of particle concentration

The dynamics adsorption of particles to the interface depends on the particles diffusivity as well as on particles concentration. In the previous sections we studied the particle charge effect on adsorption process. To investigate the effect of particle concentration, we used a series of aqueous silica nanoparticle suspensions of concentrations ranging from 0.25. 0.5 and 1wt % at two different fixed salt concentrations (0.1 and 0.05M NaCl). The concentration effect on the adsorption dynamics is showed in Fig.8. In case of 0.1M NaCl concentration, as the particles concentration increases the drop in the interfacial tension observed was more. Similar trends were observed at 0.05M NaCl. With increase in particle concentration, the number particles in the drop increase and therefore, on an average there are more particles close to the oil-water interface. As the particles surface charge in screened due to the presence of NaCl, there is more adsorption of particles to the interface with increase in particle concentration. The increased drop in the surface tension is due to increase in the particle concentration at the interface. Similar effect of particle concentration of adsorption kinetics have been reported.

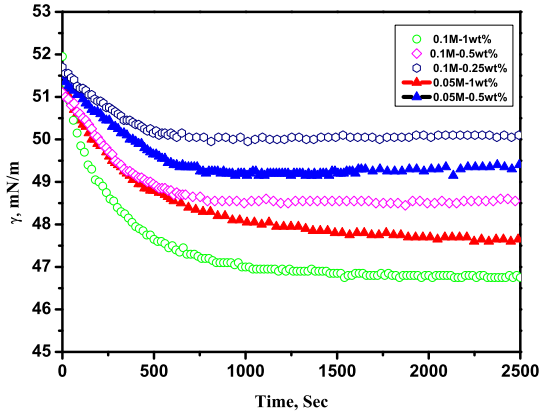

Fig. 8 The effect of particle concentration on the adsorption kinetics. The change in interfacial tension is studied for two salt concentrations (0.1M and 0.05M) by varying the particle concentration (1, 0.5 and 0.25 wt%). The interfacial tension decrease is more for high particle concentration.

4 Conclusion

In this work, we investigated the effect of particle charge and concentration on the adsorption dynamics of silica nanoparticles to the fluid-fluid interface. The experiments were conducted by considering a water drop containing monodispersed silica nanoparticle and decane as oil medium. The charge of particles and the interface was controlled by the addition of NaCl. The adsorption of particles was monitored with a pendant drop tensiometer by recording the interfacial tension as a function of time. The interfacial tension decreased was more when the particles were weakly charged, i.e more number of particles were adsorbed to the interface. When the particles were highly charged, the interfacial tension change was negligible - that is - no adsorption of particles to the interface. We modeled the early stage DST data using the WT theory. From the model we calculated the effective diffusivity of the particles at different salt concentration. We show that the change in the effective diffusivity is due to the energy barrier as the particles approach near the interface. The energy barrier estimated from DST data corroborates well with the energy barrier calculated from the overall DLVO interactions taking into account the image charge effect. When the particles are highly charged, a high net energy barrier prevents the adsorption of particles to the interface. When the particle charge was screened with sufficient NaCl, the net energy barrier decreases considerably and hence the particles readily adsorb to oil-water interface. With increase in particle concentration, there was pronounced drop in interfacial tension suggesting an increase in the population of particles at the oil-water interface. We conclude that the image charge interactions play an important role in adsorption of particles to interface and these studies will have implications on the use of particles for stabilization of incompatible interfaces.

References

1 H. Wang, V. Singh and S. H. Behrens, *The Journal of Physical Chemistry Letters*, 2012, **3**, 2986–2990.

2 B. Binks and S. Lumsdon, *Langmuir*, 2001, **17**, 4540–4547.

3 B. Madivala, S. Vandebril, J. Fransaer and J. Vermant, *Soft Matter*, 2009, **5**, 1717–1727.

4 A. B. Pawar, M. Caggioni, R. Ergun, R. W. Hartel and P. T. Spicer, *Soft Matter*, 2011, **7**, 7710–7716.

5 J. Wang, F. Yang, J. Tan, G. Liu, J. Xu and D. Sun, *Langmuir*, 2009, **26**, 5397–5404.

6 A. Stocco, E. Rio, B. P. Binks and D. Langevin, *Soft Matter*, 2011, **7**, 1260–1267.

7 B. P. Binks and T. S. Horozov, *Angewandte Chemie*, 2005, **117**, 3788–3791.

8 B. P. Binks, R. Murakami, S. P. Armes, S. Fujii and A. Schmid, *Langmuir*, 2007, **23**, 8691–8694.

9 S. Fujii, P. Iddon, A. Ryan and S. Armes, *Langmuir*, 2006, **22**, 7512–7520.

10 J. W. Tavacoli, J. H. J. Thijssen, A. B. Schofield and P. S. Clegg, *Advanced Functional Materials*, 2011, **21**, 2020–2027.

11 M. N. Lee, J. H. Thijssen, J. A. Witt, P. S. Clegg and A. Mohraz, *Advanced Functional Materials*, 2013, **23**, 417–423.

12 J. W. Tavacoli, J. H. Thijssen, A. B. Schofield and P. S. Clegg, *Advanced Functional Materials*, 2011, **21**, 2020–2027.

13 R. Aveyard, J. H. Clint, D. Nees and V. N. Paunov, *Langmuir*, 2000, **16**, 1969–1979.

14 W. Chen, S. Tan, T.-K. Ng, W. T. Ford and P. Tong, *Physical review letters*, 2005, **95**, 218301.

15 B. Madivala, J. Fransaer and J. Vermant, *Langmuir*, 2009, **25**, 2718–2728.

16 A. Würger, *EPL (Europhysics Letters)*, 2006, **75**, 978.

17 T. S. Horozov, R. Aveyard, J. H. Clint and B. P. Binks, *Langmuir*, 2003, **19**, 2822–2829.

18 V. R. Dugyala and M. G. Basavaraj, *The Journal of Physical Chemistry B*, 2015, **119**, 3860–3867.
19 N. Bizmark, M. A. Ioannidis and D. E. Henneke, *Langmuir*, 2014, **30**, 710–717.
20 O. S. Deshmukh, D. van den Ende, M. C. Stuart, F. Mugele and M. H. Duits, *Advances in colloid and interface science*, 2014.
21 K. Du, E. Glogowski, T. Emrick, T. P. Russell and A. D. Dinsmore, *Langmuir*, 2010, **26**, 12518–12522.
22 S. Ferdous, M. A. Ioannidis and D. Henneke, *Journal of Nanoparticle Research*, 2011, **13**, 6579–6589.
23 V. Garbin, J. C. Crocker and K. J. Stebe, *Langmuir*, 2011, **28**, 1663–1667.
24 N. Glaser, D. J. Adams, A. Böker and G. Krausch, *Langmuir*, 2006, **22**, 5227–5229.
25 A. Nelson, D. Wang, K. Koynov and L. Isa, *Soft matter*, 2015, **11**, 118–129.
26 Z. Sun, T. Feng and T. P. Russell, *Langmuir*, 2013, **29**, 13407–13413.
27 S. Kutuzov, J. He, R. Tangirala, T. Emrick, T. Russell and A. Böker, *Physical Chemistry Chemical Physics*, 2007, **9**, 6351–6358.
28 A. Ward and L. Tordai, *The Journal of Chemical Physics*, 1946, **14**, 453–461.
29 T. D. Gurkov, *Colloid and Polymer Science*, 2011, **289**, 1905–1915.
30 F. Ravera, L. Liggieri and A. Steinchen, *Journal of Colloid and Interface Science*, 1993, **156**, 109 – 116.
31 L. Liggieri, F. Ravera and A. Passerone, *Colloids and surfaces A: physicochemical and engineering aspects*, 1996, **114**, 351–359.
32 S. N. Moorkanikkara and D. Blankschtein, *Journal of colloid and interface science*, 2006, **296**, 442–457.
33 B. P. Binks, L. Isa and A. T. Tyowua, *Langmuir*, 2013, **29**, 4923–4927.
34 R. Aveyard, B. P. Binks and J. H. Clint, *Advances in Colloid and Interface Science*, 2003, **100**, 503–546.
35 P. A. Wierenga, M. B. Meinders, M. R. Egmond, F. A. Voragen and H. H. de Jongh, *Langmuir*, 2003, **19**, 8964–8970.
36 K. B. Song and S. Damodaran, *Langmuir*, 1991, **7**, 2737–2742.
37 S. G. Kluijtmans, E. H. de Hoog and A. P. Philipse, *The Journal of chemical physics*, 1998, **108**, 7469–7477.
38 K. Marinova, R. Alargova, N. Denkov, O. Velev, D. Petsev, I. Ivanov and R. Borwankar, *Langmuir*, 1996, **12**, 2045–2051.
39 S. Bhattacharjee and M. Elimelech, *Journal of colloid and interface science*, 1997, **193**, 273–285.
40 S. Lin and M. R. Wiesner, *Langmuir*, 2010, **26**, 16638–16641.